AN ARTIFICIAL NEURAL NETWORK BASED POWER SYSTEM STABILIZER FOR MULTI-MACHINE POWER SYSTEM

Dr. Z.S. El-Razaz* and Eng. M. Abd El-hameed

Electrical Power & Machine Department
Faculty of Engineering, Zagazig University
Zagazig, Egypt

الخلاصـة :

تـمَّ في هذا البحث اقتراح و بناء مقرر لأنظمة القدرة الكهربية باستخدام الشبكات العصبية. و قد أُخذ في الاعتبار التغير في أحوال الشبكة و كذلك التغير في نوعية الحمل الكهربي. استُخدِمَ مقرر الأنظمة لزيادة اضمحلال الذبذبات الكهربية التي تنتج عن أي اضطراب في النظام. و من عيوب استخدام مقرر ذي مكونات ثابتة أنه لا يعطي تأثيراً جيداً عند استخدامه في أحوال تختلف عن التي تم بناؤه عندها. و لذلك يمتاز المقرر المقترح بتغير قيم مكوناته عند التغير في أحوال الشبكة مما يعطي درجة أداءٍ أفضل من سابقه.

و لقد تم اختبار المقرر باستخدام أحوال أخرى لم تدخل في عملية بنائه و قد أعطى نتائج جيدة. و تم اختبار المقرر المقترح على شبكة كهربية تحتوي مولدات متعددة و أعطى نتائج جيدة .

*Address for correspondence:
Electrical Power & M/C Dept.
Faculty of Engineering
Zagazig University
P.O. Box 44514
Zagazig, Egypt
e-mail: zaglol_elrazaz@hotmail.com

ABSTRACT

An adaptive power system stabilizer (PSS) over a wide range of operating conditions and typical local load models is proposed, using an artificial neural network ANN. The PSS with fixed parameters, which improves the power system damping for one operating point, may become unsatisfactory for another one especially for a wide range of operating conditions and load models. To improve the damping of the system over a wide range of operating conditions, it is desirable to adapt the parameters of the PSS in real time, based on operating points and load models. In order to do this, on-line measurement of operating points and load model parameters are chosen as the input signals to the neural network. The outputs of the neural network are the desired parameters of the PSS. The neural network, once trained by a set of input–output patterns in the training set, can yield proper PSS parameters under any operating conditions and local load model. Simulation results show that the tuning parameters of the PSS using the ANN approach can provide better damping than a fixed-parameters PSS over a wide range of operating points and typical load models. The proposed PSS is implemented for a multi-machine system.

AN ARTIFICIAL NEURAL NETWORK BASED POWER SYSTEM STABILIZER FOR MULTI-MACHINE POWER SYSTEM

1. INTRODUCTION

As a power system stabilizer (PSS) has the ability to provide damping for lower frequency oscillations in power systems, it has been used in modern power systems [1]. Much attention has been devoted to increasing the performance of PSS. Initially, linear control theory was introduced in PSS design. Later, optimal control theory was used. Experimental results show that PSS works very well at the operating point at which the linearized model was derived [2]. However, as power systems are nonlinear systems, it is impossible for the system to always run at the pre-selected operating point. When the system is away from the specified operating point, the performance of the PSS will be different.

In recent years there have been new approaches for PSS design, using modern control techniques. Many of these approaches lack one or more of the important features that a PSS should have, *i.e.*, simplicity of structure, fast action, and adaptability [3].

One other important aspect is the effect of load models. Over time, the load model of a power system changes, and a PSS with fixed parameters designed for one load model cannot maintain the same quality with another load model [4]. It became clear that assumptions regarding load model can impact predicted system performance as significantly as the models chosen for excitation systems and synchronous machines [2].

Neural networks have been recently applied in many areas of power systems [5]. Artificial Neural Network (ANN) technology offers great potential in power system stability control. ANNs are adaptive; normally they are trained over the full working range of the controlled plant with a wide spectrum of operating conditions. A properly trained ANN can provide the desired control effect when the plant changes. Due to its parallel structure, the computation time of an ANN controller can be much shorter than for other control schemes, such as adaptive control [3].

In many cases of interconnected systems, machines are located electrically close to each other and interaction between the different system modes can occur [6].This interaction between modes is of importance, since it may result in reduction of damping of natural mechanical oscillation. Moreover, unstable oscillations may occur due to interactions among large groups of generators. In this paper, an ANN PSS is proposed to cover a wide range of operating conditions and load models.

2. SYSTEM UNDER STUDY

Consider a multi-machine system [7], as shown in Figure 1, which is a three-machine nine-bus system, including three constant-impedance loads and local non-linear loads at bus #1.

Each generator is represented by the third-order model and is equipped with a static exciter. Electromechanical equations of each generator including an static exciter are:

$$\Delta \dot{E}'_q = \frac{-1}{\tau'_{d0}} \Delta E'_q + \frac{1}{\tau'_{d0}} \Delta E_{fd} + \frac{x_d - x'_d}{\tau'_{d0}} \Delta I_d \tag{1}$$

$$\Delta \dot{\omega} = \frac{1}{\tau_j} (\Delta T_m - \Delta T_e) \tag{2}$$

$$\Delta \dot{\delta} = \omega_B \Delta \omega \tag{3}$$

$$\Delta \dot{E}_{fd} = \frac{-1}{\tau_a} \Delta E_{fd} - \frac{k_a}{\tau_a} \Delta v_f - \frac{k_a}{\tau_a} \Delta v_t + \frac{k_a}{\tau_a} \Delta v_s \tag{4}$$

$$\Delta\dot{v}_f = \frac{-k_f}{\tau_a\tau_f}\Delta E_{fd} - \left(\frac{1}{\tau_f} + \frac{k_a k_f}{\tau_a\tau_f}\right)\Delta v_f - \frac{k_a k_f}{\tau_a\tau_f}\Delta v_t + \frac{k_a k_f}{\tau_a\tau_f}\Delta v_s \ , \tag{5}$$

where Equations 4 and 5 represent the static exciter state equations. System data is given in the Appendix.

3. NON-LINEAR LOAD MODEL

A nonlinear load model which represents the power relationship to voltage as an exponential equation:

$$\frac{p_l}{p_{l0}} = \left(\frac{v_t}{v_{t0}}\right)^{a_p} \quad \frac{q_l}{q_{l0}} = \left(\frac{v_t}{v_{t0}}\right)^{a_q} , \tag{6}$$

where p_l and q_l are the load active and reactive power respectively; v_t is the load bus voltage; a_p and a_q are constants representing the parameters of the load models; and p_{l0}, q_{l0}, and v_{t0} are the nominal values prior to a disturbance. Constant current and constant impedance are special cases of the exponential model.

4. BLOCK DIAGRAM SIMULATION

All the system components (synchronous machine, exciters, and stabilizers) can be combined into a block diagram. This diagram represents the LAPLACE transform of the differential equations. Also, the algebraic equations are reduced and represent the tying between each machine through the reduced admittance matrix of the system network.

Due to its simplicity and flexibility, the system has been modeled using the SIMULINK toolbox in MATLAB. Separate methodology using state space representation has been used to verify the results obtained from the SIMULINK.

5. STEADY STATE STABILITY EVALUATION AND MODES IDENTIFICATION

The eigenvalues of the system state space matrix are indicative of the system performance. Mode identification is needed to relate each eigenvalue to its corresponding state variable. This is important to figure out which state variables contribute largely to the system instability.

The participation matrix method has been used to identify the correlation between system states and modes [8]. The significant elements (related to the mechanical modes) of the participation matrix are given in Table 1.

This table indicates strong participation from machine #1 and machine #2 into the first mode (0.33 Hz). This mode can be considered as an interarea mode. The third mode frequency in the first row of the Table has a frequency of approximately 1.67 Hz. The participation factors indicate a strong contribution from the third machine into this mode,

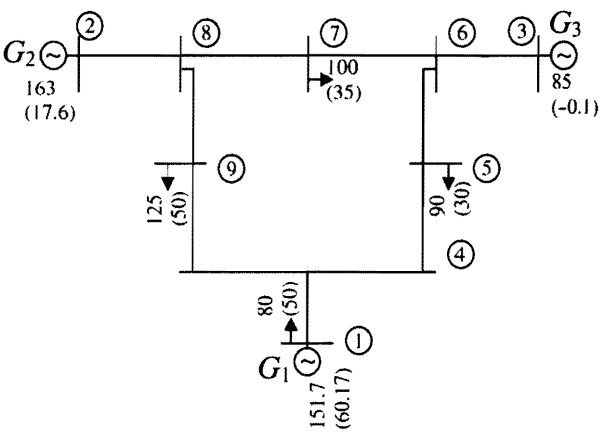

Figure 1. System under study.
P *and* Q *are in MW and MVAR.*

with very weak contributions from machines #1 and #2. Consequently, one may consider this mode as a local mode [6]. This can be expected since machine #3 has a small rating as compared to the others. This mode has not been considered in designing the PSS since it has quite a large stability margin.

System eigenvalues after mode identification are shown in Table 2; eigenvalues corresponding to the torque-angle loop of machine #1 are unstable at this operating condition since the real part is positive.

6. EFFECT OF A NON-LINEAR LOCAL LOAD ON SYSTEM PERFORMANCE

The accurate modeling of loads is a difficult task for several reasons [9]. The large number of diverse load components and ownership and location of load devices in customer facilities are among these reasons. Lack of precise information on the composition of loads, and uncertainties regarding the characteristics of many load components are other causes of this difficulty. Consequently, an approximate model will be quite useful. This can be obtained by measuring the system variables (P, Q, and V) at certain substations where a composite non-linear load exists.

To study the effect of the nonlinear load, a local load at bus #1 will be treated as a local non-linear load. This will be considered in forming the matrices of the state space model of the system. System eigenvalues with different load parameters are shown in Table 3. From this Table, a considerable change in the eigenvalues corresponding to the torque-angle loop of machine one is observed. The real part changes from 0.06 to 0.11 when the load model changes from constant impedance to constant active power, while the torque-angle loop eigenvalues of machines #2 & 3 are almost unchanged. This indicates that for designing a PSS, it is enough to consider the local non-linear load for the nearest generator [9].

It is important to stress that non-linear loads other than the constant impedance contribute more negative damping to system performance [9], as shown in Figure 2. The change in the active power index affects largely the real part of the

Table 1. The Participation Matrix.

x λ	$0.07 \pm j1.99$	$-0.42 \pm j7.47$	$-0.71 \pm j10.52$
$\Delta\delta_1$	0.313	0.154	0.004
$\Delta\delta_2$	0.104	0.31	0.097
$\Delta\delta_3$	0.053	0.057	0.406

Table 2. System Eigenvalues.

System states		λ_i
Torque angle loop	$\Delta\omega_1, \Delta\delta_1$	$0.07 \pm j1.99$
	$\Delta\omega_2, \Delta\delta_2$	$-0.42 \pm j7.47$
	$\Delta\omega_3, \Delta\delta_3$	$-0.71 \pm j10.52$
Interaction modes		-3.49
		-1.5
		$-0.75 \pm j0.87$
		$-1.43 \pm j0.66$
Exciters modes		-215.64
		-218.39
		-218.88

mode as well as the proportional part of the PI stabilizer (as will be seen later). On the other hand, the effect of changing a_q is much smaller as compared with a_p. Consequently, in choosing the data distribution for the ANN training, a larger step is used for a_q (0.4) as compared to that of a_p (0.2).

7. PI PSS DESIGN

The excitation system with the associated PI PSS is shown in Figure 3. Here, τ_w is the washout time constant, and k_p and k_I are the gain settings of PI PSS.

The state-variables model of the system is expressed as:

Table 3. System Modes for Different Load Parameters.

System states		λ_i ($a_p = 2$, $a_q = 2$)	λ_I ($a_p = 0$, $a_q = 2$)
Torque angle loop	$\Delta\omega_1$, $\Delta\delta_1$	$0.06 \pm j2.03$	$0.11 \pm j2.02$
	$\Delta\omega_2$, $\Delta\delta_2$	$-0.42 \pm j7.4$	$-0.42 \pm j7.47$
	$\Delta\omega_3$, $\Delta\delta_3$	$-0.71 \pm j2.0$	$-0.71 \pm j10.52$
Interaction modes		-3.52	-3.54
		-1.51	-1.5
		$-0.75 \pm j0.8$	$-0.75 \pm j0.87$
		$-1.41 \pm j0.6$	$-1.4 \pm j0.59$
Exciters modes		-215.54	-215.55
		-218.39	-218.37
		-218.88	-218.88

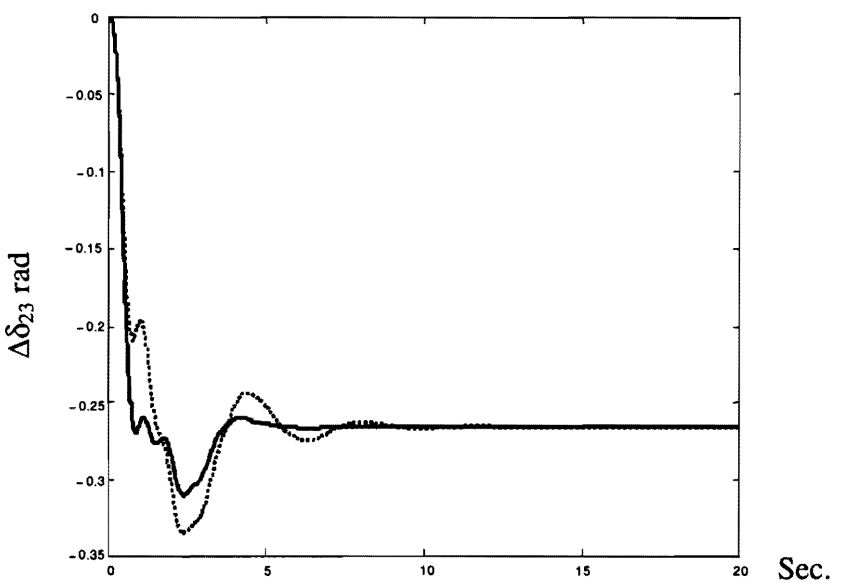

Figure 2. Response of $\Delta\delta_{23}$ at different load models for 0.1 step change in E_{ref1}.

—— *Constant impedance* $a_p = a_q = 2$

····· *Constant power* $a_p = 0.0$ *and* $a_q = 2.0$.

$$X(t) = AX(t) + BU(t)$$

$$Y(t) = CX(t), \tag{7}$$

where $X(t) = [\Delta E'_{q1}, \Delta\omega_1, \Delta\delta_1, \Delta E_{fd1}, \Delta v_{f1}, \Delta E'_{q2}, \Delta\omega_2, \Delta\delta_2, \Delta E_{fd2}, \Delta v_{f2}, \Delta E'_{q3}, \Delta\omega_3, \Delta\delta_3, \Delta E_{fd3}, \Delta v_{f3}]$ is the state variable vector, $Y = \Delta\omega_1$ is the output signal, and $U = \Delta v_s$ is the control signal to the excitation system.

The system matrix A is a function of the operating point as well as of the load model parameters (a_p, a_q). The matrices B and C are given as:

$$B = \left[0 \;\; 0 \;\; 0 \;\; \frac{k_a}{\tau_a} \;\; \frac{k_a k_f}{\tau_a \tau_f} \;\; 0 \;\; 0 \;\; 0 \;\; 0 \;\; 0 \;\; 0 \;\; 0 \;\; 0 \;\; 0 \;\; 0\right]^T,$$

$$C = [0 \;\; 1 \;\; 0 \;\; 0 \;\; 0 \;\; 0 \;\; 0 \;\; 0 \;\; 0 \;\; 0 \;\; 0 \;\; 0 \;\; 0 \;\; 0 \;\; 0].$$

Also, $Y(s) = H(s)^* U(s)$.

The dynamic equation for the PSS is defined as: $Y_{PSS}(s) = H_{PSS}(S) U_{PSS}(s)$

where

$$H_{PSS}(s) = \frac{s\tau_w}{1 + s\tau_w}\left(k_p + \frac{k_I}{s}\right)$$

and

$$Y_{PSS} = \Delta V_s, \qquad U_{PSS} = \Delta\omega = Y(s).$$

By replacing $S = \lambda$, the following equation can be derived using the modal control theory,

$$H_{PSS}(\lambda) = \frac{1}{C(\lambda I - A)^{-1} B} = \frac{\lambda\tau_w}{1 + \lambda\tau_w}\left(k_p + \frac{k_I}{\lambda}\right) = H^{-1}\lambda. \tag{8}$$

The gains k_p and k_I of the PI PSS can be determined by substituting a pair of the prescribed mechanical mode eigenvalues $\lambda_{1,2}$ into the last equation, so we have a pair of algebraic equations with two unknowns k_p, k_I.

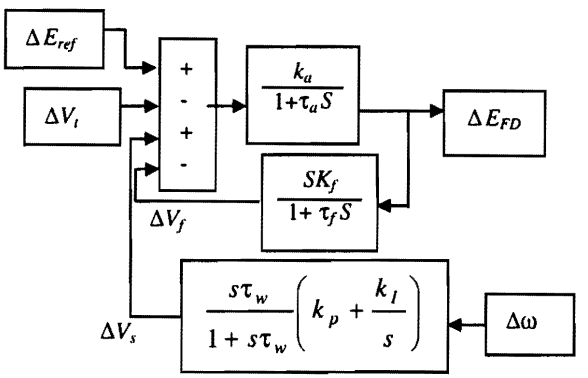

Figure 3. Static exciter with a PI PSS.

8. SYSTEM RESPONSE BEFORE ADDING THE PI PSS

Response of $\Delta\delta_{12}$ to a step change in the reference input to the static exciter of machine #1 before adding the stabilizer is shown in Figure 4. From this, the system instability is clear, since the response increases continuously with time. The inter-machine oscillation which may be consider as inter-area oscillation at a frequency of 0.5 Hz is clearly observed in this Figure. Each of the machines at bus #1 and that at bus #2 can be considered an area by itself. This is mainly justified by the electric distance between them, and their ratings. The local oscillation can be observed if another machine is installed at bus 1 near to machine #1. Mode oscillation within each machine can be observed by considering the response E'_{q1} state within the machine at bus #1. The system configuration can be changed to allow the different multi-modes (inter-plant, local, inter-area) to appear.

If the new location for the pair of mechanical mode eigenvalues $\lambda_{1,2}$ is selected to be $-2 \pm j2$, then the gain setting k_p, k_I for the PI PSS can be computed using last equation, and the results are as follows: $K_p = 12.4483$, $K_I = 240.8451$.

The eigenvalues of the closed-loop system (system with PI PSS) are given in Table 4 ($a_p = a_q = 2$), it is found that the prescribed mechanical mode eigenvalues $\lambda_{1,2}$ are exactly assigned. Considerable improvement in system damping can be expected in view of the eigenvalues in Table 4.

9. PERFORMANCE OF THE SYSTEM WITH THE PI PSS

System responses $\Delta\delta_{12}$ (when $\lambda_{1,2} = -2 \pm j2$) to a step change in the reference input to the static exciter of machine #1 is shown in Figure 5. The ANN PSS damped out the inter-machine mode ($f = 0.5$ Hz) oscillation very effectively even by using one controller.

10. EFFECT OF OPERATING CONDITIONS AND THE LOCAL NON-LINEAR LOAD ON SYSTEM PERFORMANCE

To obtain good damping characteristics for the system over a wide range of operating points and load models, the PI PSS gains k_p and k_I must be adapted to prevent the desired mechanical-mode eigenvalues $\lambda_{1,2} = -2 \pm j2$ from drifting. The computed gains (k_p, k_I) for some typical load models at the base case operating conditions are listed in Table 5. Also, the data in Table 6 represent a small sample of the data used. In this table, the machine operating condition is changed, with fixed load model. Table 6 indicates a boundary operating condition ($P = 2.5$) for the first machine. This is used only as an extreme data for training the ANN but is not by any means an actual operating condition.

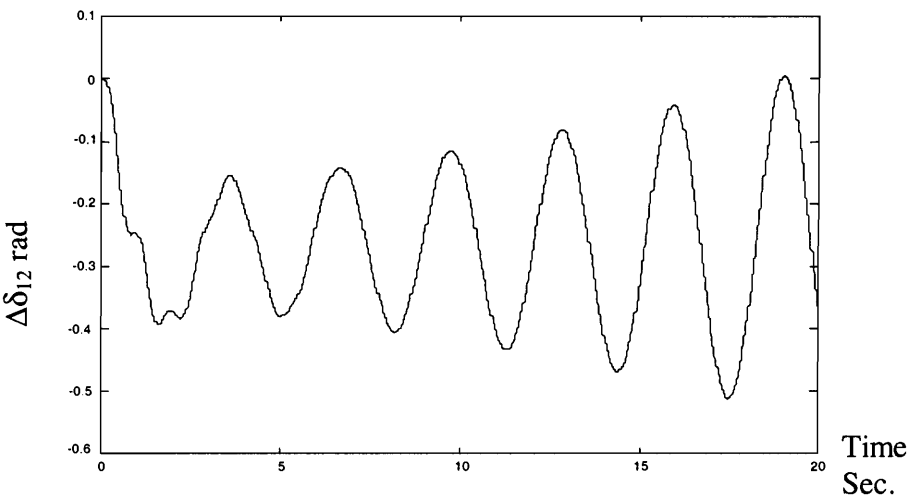

Figure 4. Response $\Delta\delta_{12}$ to 0.1 p.u. step change in ΔE_{ref1}.

11. ANN PSS STRUCTURE

ANN will be used to derive the PI PSS by calculating its suitable gains (k_p, k_I) for any operating point and local load model. So the inputs to the ANN are (p_{g1}, q_{g1}, p_{g2}, q_{g2}, p_{g3}, q_{g3}, a_p, a_q), and the outputs are (k_p, k_I). Most of the authors in the literature used $\Delta\omega$, $\Delta\dot{\omega}$ as inputs to the ANN PSS. In this work, p, q and the non-linear load parameters are used. It is important to note that the change in $\Delta\omega$ and $\Delta\dot{\omega}$ are functions in these variables. Choosing p, q and load parameters gives direct feeling to the engineer about system conditions. Reference [10] used p, q and the machine voltage as inputs to the NEURO-FUZZY controller to damp the local modes of oscillations over a wide range of operating conditions. The authors in this reference did not study the effect of the nonlinear load. Also, the authors used specified damping ratio to obtain the data needed to train their controller. In this work we used pole-placement technique which has similar effect. Also the nonlinear load parameters are used as inputs to the controller.

Table 4. System Modes with the PI PSS.

System states		Closed loop system (with PI PSS)	Damping Ratio ζ
Torque angle loop	$\Delta\omega_1$, $\Delta\delta_1$	$-2 \pm j2$	0.707
	$\Delta\omega_2$, $\Delta\delta_2$	$-0.28 \pm j7.43$	0.0376
	$\Delta\omega_3$, $\Delta\delta_3$	$-0.71 \pm j10.5$	0.067
Interaction modes		$-0.61 \pm j1.95$	0.298
		$-0.75 \pm j0.87$	0.6529
		$-1.13 \pm j0.41$	0.94
Exciters modes		-215.55	1
		-218.41	1
		-218.88	1
Stabilizer mode		-10.5	1

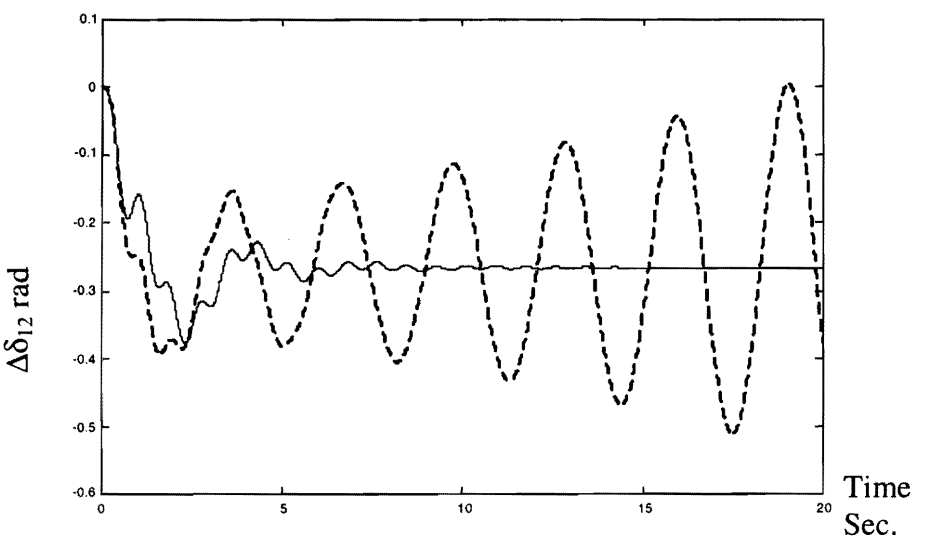

Figure 5. Response $\Delta\delta_{12}$ before and after the PI PSS.
—— With PI PSS ----- Without PI PSS.

12. NETWORK TRAINING

The multilayer feedforward network used in this work is trained using the backpropagation (BP) paradigm. The BP algorithm uses the supervised training technique. In this technique, the interlayer connection weight and the processing elements thresholds are first initialized to small random values. The network is then presented with a set of training patterns (input–output). Two methods are used to improve backpropagation algorithm, which are: Learning with momentum and adaptive learning rate.

13. DATA PREPARATION

Before the ANN model can be used to derive the desired output, the model has to be trained to recognize the relationship between the input parameters, and the desired power system stabilizer gains. The gains are obtained by the pole-placement for each operating condition. All the computations are performed off-line. The input data set has to cover as far as possible the operating range, including lag and lead conditions and the generation level of each machine. The load parameters a_p, a_q ranges used are between 0 and 4. Training data consists of 45 input–output patterns.

Patterns within these ranges are evenly distributed so that the training can cover all possible operating conditions and typical load values. If it is not the case, training will tend to focus on regions where training patterns are densely clustered, and neglect those that are sparsely populated, hence, producing inaccurate gains.

For the present work, the training process was performed using MATLAB. The network converged to a sum square error (SSE) of 0.0049 with 18 neurons in the hidden layer. Having trained the network successfully, the next step is to test the trained network using test data.

Table 5. The Computed Gain Settings k_p and k_I for Different Load Models.

Load model		Gain settings	
a_p	a_q	k_p	k_I
0.0	0.0	-10.9197	246.91
0.2	0.0	-6.5313	251.2602
0.2	0.4	-27.3555	197.377
2.0	2.0	12.4483	240.8457
0.0	2.0	-21.4168	219.0884
2.0	0.0	21.6581	260.6058
1.0	1.0	3.3429	249.2448

Table 6. The Computed Gain Settings k_p, k_I for Different Operating Conditions ($a_p = a_q = 2$).

P_{g1}	Q_{g1}	P_{g2}	Q_{g2}	P_{g3}	Q_{g3}	K_p	k_I
1.51	0.60	1.63	0.17	0.85	-0.001	12.4	240
2.50	0.61	1.13	0.12	0.35	0.009	74.7	284
1.64	0.47	1.7	0.04	0.95	-0.54	-0.26	111
1.71	0.25	1.0	0.01	1.28	-0.2	12.6	75.3
0.83	0.27	1.2	-0.11	1.0	-0.224	91.9	482
1.18	-0.12	1.0	0.10	1.0	-0.007	-70	87.9
2.17	2.31	1.63	1.74	1.2	1.577	210	180

14. NETWORK TESTING AND VALIDATION

Figures 6 and 7 provide the results of testing the ANN network by a set of input patterns, and illustrate the relationship between actual and predicted gains for some operating points and load models.

To demonstrate the effectiveness of the proposed ANN-based PSS, time domain simulation were performed for the power system under a 0.1 p.u. step change in ΔE_{ref1} over a wide range of operating conditions and local load models. The superiority of the proposed ANN-based PSS can be seen from the time response of the system shown in Figure 8. It compares the response of the system when using a fixed parameter PSS, and an ANN-based PSS. This figure shows that, the settling time is reduced from 10 sec for the fixed PSS to about 6 sec for the PI ANN. Moreover, the oscillations and the overshoot for the PI ANN are less than that of the fixed PSS.

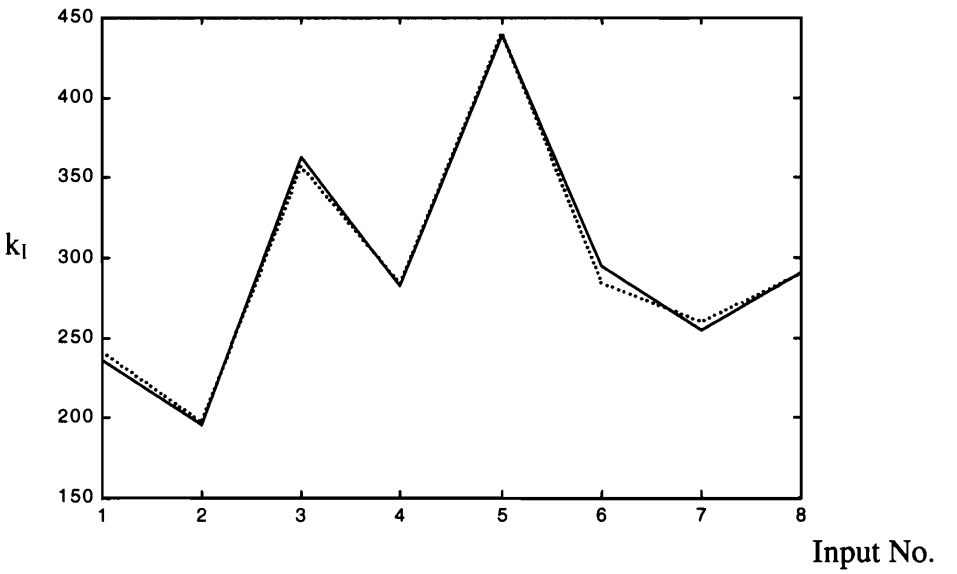

Figure 6. Actual gains vs. *the predicted gains from the ANN model for* k_I.
····· *Actual gain* —— *Predicted gain.*

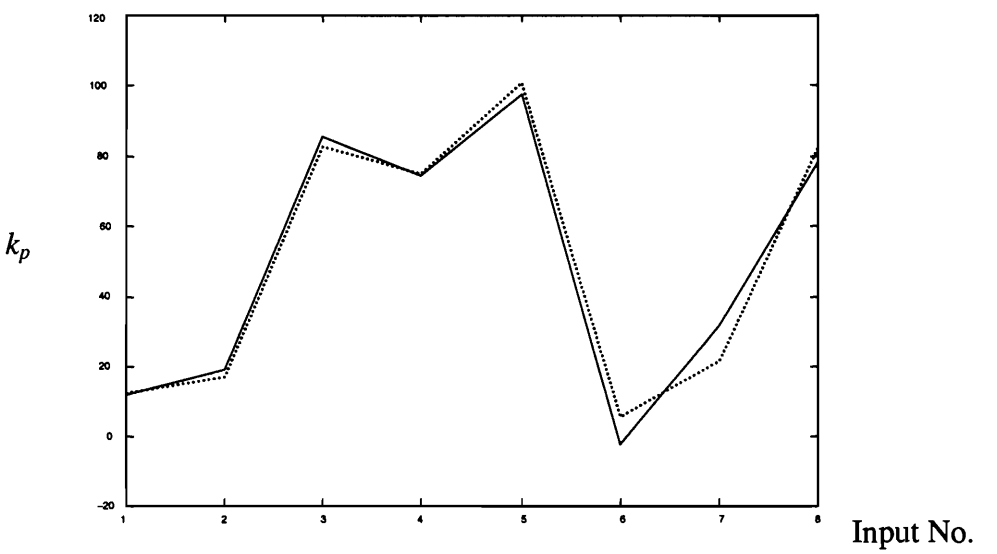

Figure 7. Actual gains vs. *the predicted gains from the ANN model for* k_p.
····· *Actual gain* —— *Predicted gain.*

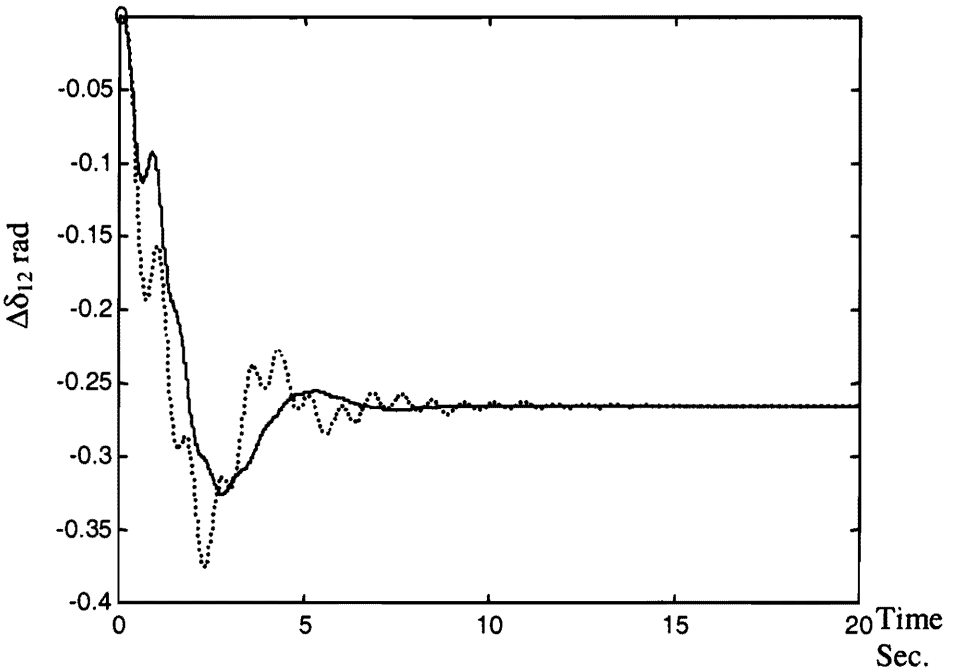

Figure 8. System response for 0.1 p.u. change in ΔE_{ref1}.
—— *ANNPSS* ····· *Fixed gain PSS.*

15. CONCLUSION

This paper illustrates the superiority of the PSS based upon ANN over the fixed PSS. The proposed PSS stabilizes the system for different operating conditions as well as various non-linear local load models. The proposed ANN PI stabilizer is tested for multi-machine power system.

REFERENCES

[1] Jan Machowski, Janusz W. Bialek, and James R. Bumby, *Power System Dynamics and Stability.* Chichester: John Wiley and Sons, 1997.

[2] K.A. Ellithy, S.M. Al-Alawi, and M.A. Choudhry, "Design of an Adaptive Power System Stabilizer Using Artificial Neural Networks", *Alazhar Engineering Fifth International Conference, Cairo, Egypt,* May 1996, pp. 14–20.

[3] Y. Zhang, G.P. Chen, O.P. Malik, and G.S. Hope, "An Artificial Neural Network Based Adaptive Power System Stabilizer", *IEEE Trans. on Energy Conversion,* **8(1)** (1993), pp. 71–84.

[4] Kerstin Linden and Inger Segerqvist, *Modeling of Load Devices and Studying Load/System Characteristics.* Goteborg, Sweden: Chalmers University of Technology Press, 1992.

[5] Mohamed A. El-Sharkawi, "Overview of Neural Network Application to Power Systems", *Record of MEPCON'97, Alexandria, Egypt,* January 1997, pp. 302–309.

[6] Y. Zhano, O.P. Malik, and G.P. Chen, " Artificial Neural Network Power System Stabilizers in Multi-Machine Power System Environment", *IEEE Trans. on Energy Conversion,* **10(1)** (1995), pp.147–155.

[7] P.M. Anderson and A.A. Fouad, *Power System Control and Stability.* Iowa: Iowa State University Press, 1977.

[8] Y.Y. Hsu and C.L. Chen, " Identification of Optimum Location for Stabilizer Application Using Participation Factors", *IEE Proc. C,* **134(3)** (1987), pp. 238–244.

[9] J.V. Milanovic and I.A. Hiskens, "Oscillatory Interaction Between Synchronous Generator and Local Voltage-Dependent Load", *IEE Proc. — Gener. Transm. Distrib.*, **142(5)** (1995), pp. 473–480.

[10] M.A. Abido and Y.L. Abdel-Magid, " A Hybrid Neuro-Fuzzy Power System Stabilizer for Multi-Machine Power System", *IEEE Trans. on Power Systems,* **1(4)** (1998), pp. 1323–1330.

APPENDIX

The system parameters and operating conditions (100 MVA base) are [7]:

Generator:

	H (sec)	X_d (pu)	X_q (pu)	X'_d (pu)	τ'_{d0} (sec)
$G(1)$	23.64	0.146	0.0969	0.068	8.96
$G(2)$	6.4	0.8958	0.8645	0.1198	6.00
$G(3)$	3.01	1.3125	1.2578	0.1813	5.89

Exciter:

	K_a	τ_a (sec)	K_f	τ_f (sec)	
$G(1)$	400	0.05	0.025	1.0	
$G(2)$	400	0.05	0.025	1.0	
$G(3)$	400	0.05	0.025	1.0	

Transmission line:

Line #	Fr.	To	R(pu)	X(pu)	$B/2$(pu)
1	1	4	0	0.0567	0
2	2	8	0	0.0625	0
3	3	6	0	0.0586	0
4	4	6	0.01	0.085	0.176
5	4	5	0.017	0.092	0.158
6	8	9	0.032	0.161	0.306
7	5	6	0.039	0.17	0.358
8	7	8	0.008	0.072	0.149
9	6	7	0.011	0.1008	0.209

NOTATION

δ	torque angle
ω_b	synchronous speed
E_{fd}	equivalent excitation voltage
E_{ref}	reference voltage
V_t	terminal voltage
τ_j	Inertia constant
k_a, τ_a	regulator gain and time constant
E'_q	stator EMF proportional to the field flux linkage
τ'_{d0}	open circuit time constant of excitation circuit
T_m, T_e	mechanical and electrical torques.
ω	rotor speed
x'_d	d-axis transient reactance
V_f	feedback stabilizing excitation voltage
I_d	current in d-axis circuit
x_d, x_q	synchronous reactance's
$H(s)$	system transfer function
$H_{PSS}(s)$	PSS transfer function

Paper Received 30 November 1999; Revised 4 October 2000; Accepted 29 November 2000.